Chapter 13

Acronyms Anonymous II: Gradient Echo

13.1 Introduction

The other major branch of the pulse sequence family tree is **G**radient **E**cho (GE), also known as **G**radient **R**ecalled **E**cho (GRE), **F**ield **E**cho (FE) or **F**ast **F**ield **E**cho (FFE). We'll use the acronym GE. Gradient echo was originally conceived as a means of speeding up the MR acquisition, by reducing the amount of longitudinal (M_z) recovery required between successive RF excitations. Gradient-echo sequences are commonly encountered as localizer or scout planning scans, or in dynamic (with contrast) studies in the body, or for angiographic or bright blood imaging, often as three-dimensional acquisitions.

In this chapter you will learn that

- speed enhancement in GE is achieved by a combination of low flip angle and short TR, which minimizes the T_1 recovery required between successive TR periods;
- spoiled GE produces T_1, proton density (PD) or T_2^* contrast;
- water and fat images can be produced using in-phase and out-of-phase TEs;
- rewound GE gives mixed contrast depending upon the ratio of T_2 and T_1 but higher SNR than spoiled GE, and is also subject to T_2^* decay;
- time-reversed GE shows 'spin-echo' type properties giving T_2 weighting;
- k-space segmentation applied to GE results in ultra-fast acquisitions such as turbo-FLASH and GE-EPI.

To understand this chapter you need to be familiar with the material from Chapters 4, 8 and 9 and have some grasp of the concept of k-space. For each sequence examined we will answer the following questions: How fast is it? How does it localize signal? What contrast does it produce? And how does it avoid artefacts?

13.2 Image Formation in Gradient Echo

The image-formation principles of a basic GE sequence were considered in Chapter 8. The echo is formed by the dephasing and rephasing of the FID signal by the frequency-encoding gradient (refer back to Figure 8.4 for a reminder). In GE, speed is enhanced by using a small flip angle so that TR can be reduced dramatically without saturating or driving the signal to zero. After a few RF pulses the magnetization gets into a steady-state where the recovery in each TR period exactly matches the effect of the excitation as considered briefly in Chapters 3 and 4 and shown in Figure 13.1

A key point for GE is that the dephasing effects of magnet inhomogeneities and local susceptibility variations are not corrected. The MR decay signal is therefore determined by T_2^* rather than T_2, so shorter values of TE are used, generally less than 10 ms. Additionally there are interesting cancellation effects relating to water and fat signals which are peculiar to GE. We shall see that there are three main branches in the gradient-echo family tree: spoiled GE, rewound GE and time-reversed GE. Example images are shown in Figure 13.2.

The extension of spoiled and rewound GE sequences to 3D is relatively straight forward by the addition of a second ('slab direction') phase-encode gradient as we saw in Section 8.8. The scan time becomes

$$\text{Scan time} = \text{NSA} \times N_{\text{PE1}} \times N_{\text{PE2}} \times \text{TR}$$

where NSA is the number of signal acquisitions and $N_{\text{PE1,2}}$ the dimensions of the phase-encode matrices.

13.3 One Tree, Many Branches: FIDs, Echoes and Coherences

If we have a train of RF pulses with TR significantly greater than T_2 as in conventional spin echo, then the

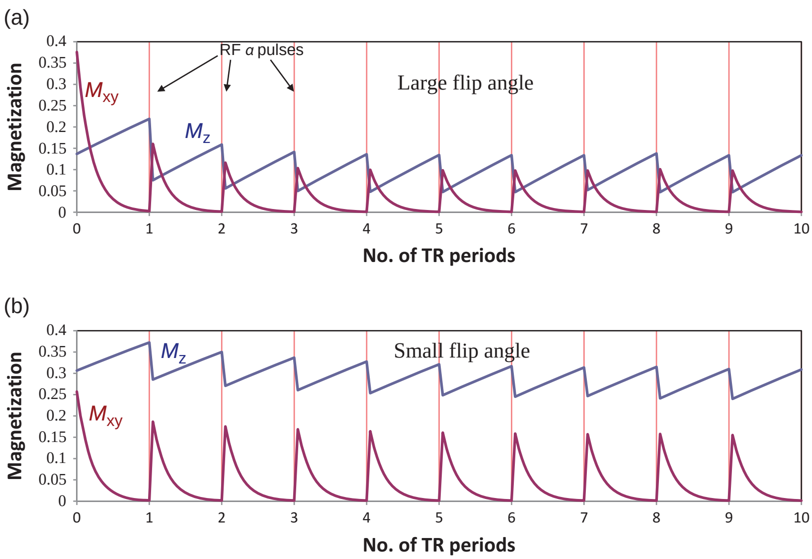

Figure 13.1 Steady-state magnetization in spoiled gradient echo. After a number of TR, a constant signal (M_{xy}) is obtained. (**a**) Large flip angle (70º), (**b**) small flip angle (40º). $TR/T_1 = 0.1$, $T_2^* = 0.02 \times T_1$.

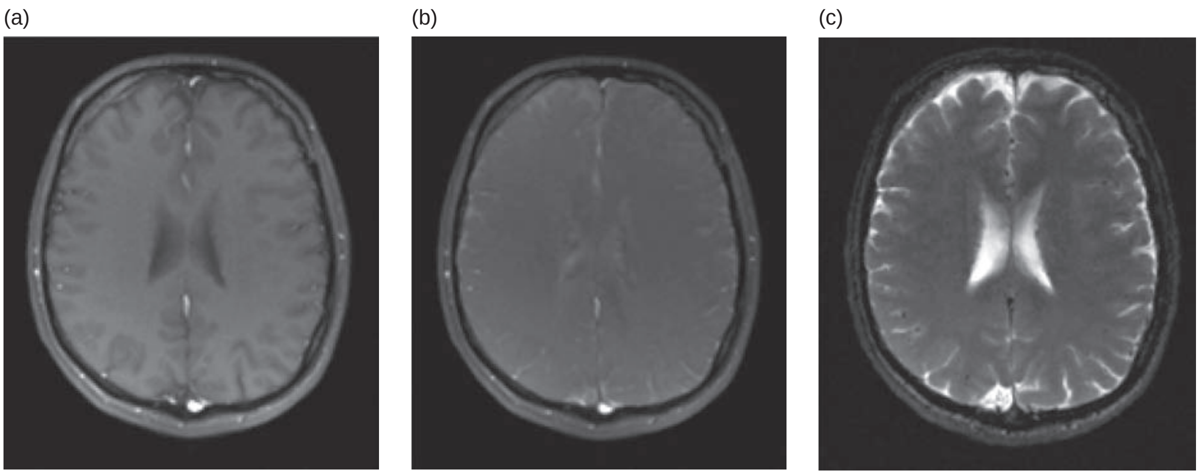

Figure 13.2 Gradient-echo images. (**a**) spoiled GE, (**b**) rewound GE, (**c**) time-reversed GE. All with TR = 20 ms, TE = 5.8 ms, flip angle $\alpha = 25°$.

transverse component of magnetization always fully decays before the onset of the next RF pulse. Each RF pulse will always be acting solely on longitudinal magnetization and the strength of the FID signal will depend mainly upon T_1. However, if TR is less than T_2 then a remnant of transverse magnetization will remain as the next RF pulse is applied. This results in 'Hahn' or partial echo formation in addition to the FID. The origin of these signals is considered in Box 'Echoes and Coherences: Hahn and Stimulated Echoes'.

Echoes and Coherences: Hahn and Stimulated Echoes

We have seen that a 90–180° pulse pair can generate a spin echo. However, any pair of RF pulses, of any flip angle (except true 180°), can form a Hahn or partial spin echo, and each echo can be further refocused by a subsequent RF pulse. The Hahn echoes are smaller in magnitude than spin echoes and have a T_2 dependence.

The formation of a Hahn echo for a pair of 90° pulses is shown in Figure 13.3. We see that it is not a fully refocused echo but that at time TE all the spin

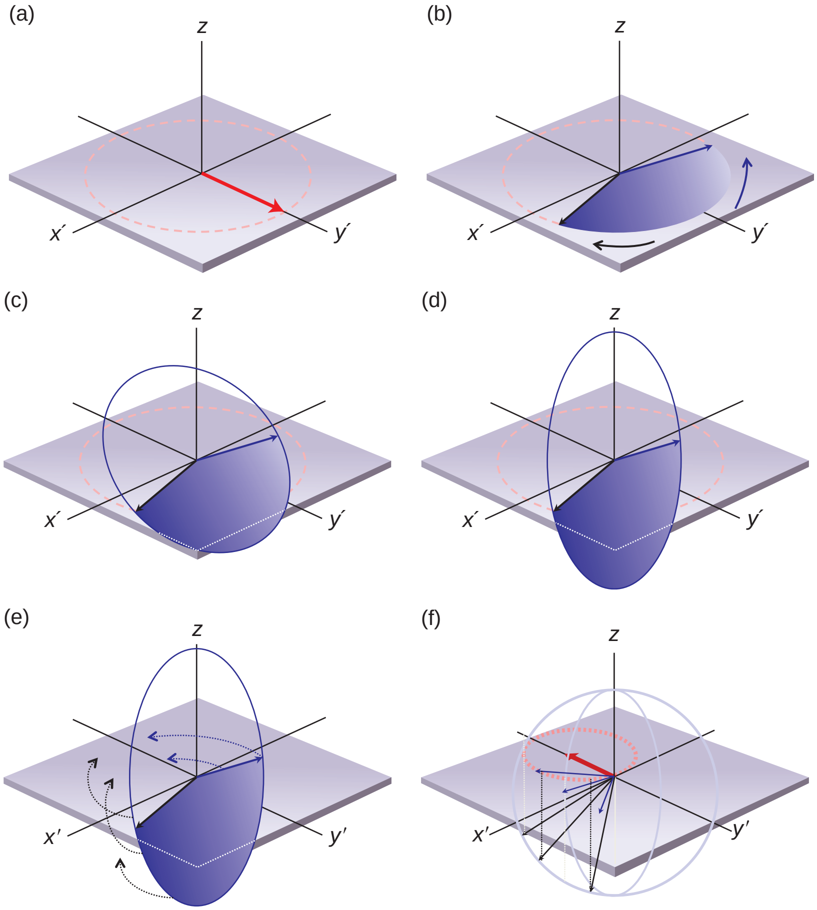

Figure 13.3 Formation of Hahn 'partial' echoes. (**a**) Transverse magnetization after first RF pulse; (**b**) immediately before the second RF pulse; (**c**) during and (**d**) immediately after this pulse; (**e**) continued transverse dephasing before the echo (**f**). The partially refocused Hahn echo occurs when all the transverse components (shadows) of the magnetization lie in a circular arrangement after a time twice the echo spacing.

vectors are of the same sign and lie in a circle, giving an echo magnitude of half of a full spin echo. For angles smaller than 90°, visualizing how the echo is formed is less intuitive. Instead of forming a circle of vectors they lie in an ellipse which refocuses less fully in the $-x'y'$ quadrant.

Stimulated echoes arise when you have three RF pulses. The first pulse generates transverse magnetization, which is 'converted' to and stored as longitudinal (T_1) magnetization by the second, and finally refocused by the third. In Figure 13.4 we see that three RF pulses will produce five echoes, three Hahn echoes from each pair of pulses, an echo created by refocusing the first echo by the third pulse and the stimulated echo. The stimulated echo has T_1 and T_2 behaviour. Its echo time with respect to the first RF pulse is

$$TE_{\mathrm{STE}} = 2 \cdot t_{\mathrm{a}} + t_{\mathrm{b}}$$

In a long RF pulse train, it is not just successive RF pulses that give rise to echoes, but each pair of pulses may do so as well. If the TR is constant, which is normal, these echoes will coincide with the wanted FID signal but, since they arose from earlier excitations, they may have different spatial encoding and contrast – and if left untended may cause artefacts.

GE sequences cope with this by either 'spoiling' the residual transverse magnetization after data acquisition and before the next RF pulse (sometimes called incoherent sequences), or by rewinding the gradients, so that the transverse magnetization at the end of each TR period has no spatial encoding. This results in a rewound (sometimes called coherent) steady-state sequence.

In a regularly spaced train of RF pulses, the echo signals will coincide with the following RF pulses and therefore add to the FID signal. How these so-called transverse coherences are dealt with determines the contrast behaviour of the sequence. 'Spoiling'

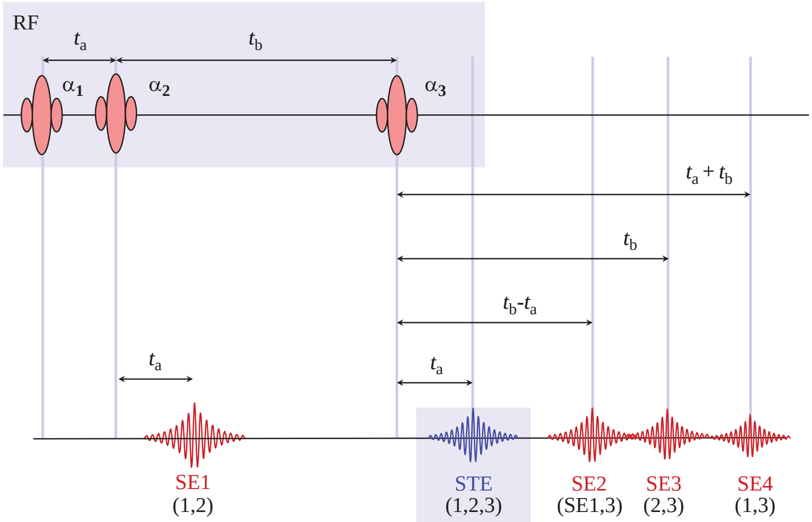

Figure 13.4 Three RF pulses may give rise to four Hahn echoes from each pair of RF pulses SE1, SE3, SE4 and the refocusing of the first echo by the third RF pulse. The stimulated echo STE is generated by all three RF pulses. The times of echo formation are given in terms of t_a and t_b, the time intervals between the RF pulses.

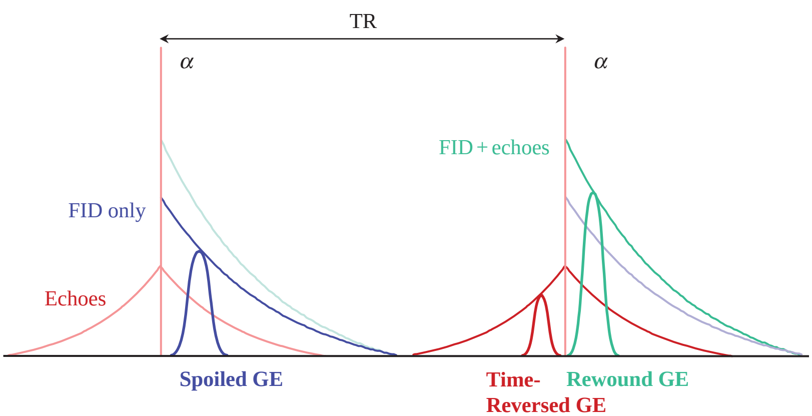

Figure 13.5 Gradient echo: coherent and incoherent signal formation in the steady state from a regular train of RF excitation pulses α.

removes the transverse coherences. ‘Rewinding’ utilizes them as signal. In time-reversed GE the echoes alone, excluding the fresh FID signal, are used in image formation. This gives us three main ways to obtain the images in Figure 13.2, illustrated in Figure 13.5, each with distinctive appearance. The relative size of the different signal components is explored further in Box ‘Echo Amplitudes’.

Echo Amplitudes

A further way of understanding coherence is to think of an RF pulse of arbitrary flip angle as acting in three separate ways, as follows.

1. Part of it acts like a 0° pulse. This means it has no effect upon either transverse or longitudinal magnetization. The relative amplitude of magnetization affected by this component is

$$M_{\text{'}0^\circ-\text{like'}} \propto \cos^2(\alpha/2)$$

2. Part acts like a 90° pulse, converting longitudinal magnetization into transverse, and transverse into longitudinal magnetization. The amplitude of this component is

$$M_{\text{'}90^\circ-\text{like'}} \propto \sin\alpha$$

3. Part of it acts like a 180° pulse, inverting pre-existing longitudinal magnetization and refocusing transverse magnetization by means of a partial or Hahn echo with amplitude

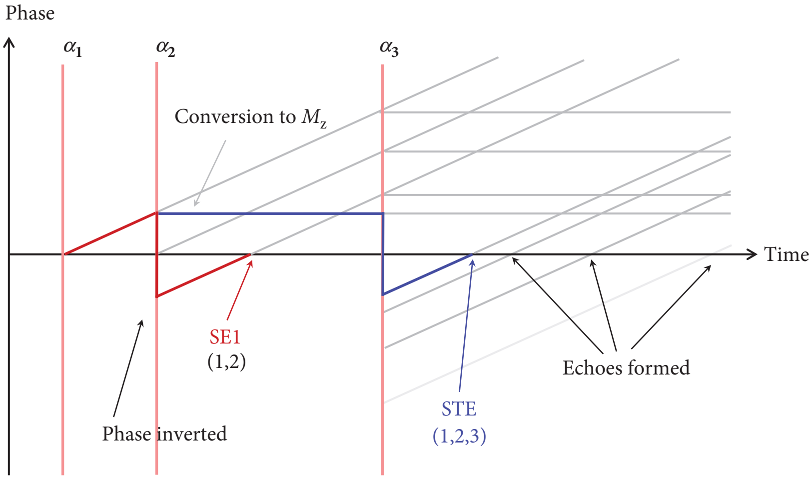

Figure 13.6 Coherence pathway diagram showing the formation of the first spin echo (red line), the stimulated echo (blue) and all the other echoes (grey).

$$M_{'180^\circ-\text{like}'} \propto \sin^2(\alpha/2)$$

From this, one can predict that the Hahn echo from two 90° pulses will have half the amplitude of a spin echo. Similarly, a true 180° pulse will only invert or refocus, and not cause partial or stimulated echoes, but we can predict that an imperfect 180° pulse will cause unwanted components of magnetization. The nature of the slice profile means that such imperfections will almost always exist for a selective refocusing pulse. This was a source of potential artefact in TSE but is avoided by using phase rewinder gradients before each 180° pulse so that any partial or stimulated echo components are properly spatially encoded.

Rewound GE sequences contain components from transverse coherences and FID and give mixed contrast depending upon the ratio of T_2 and T_1. They are also subject to T_2^* decay. Time-reversed GE sequences use just the transverse coherence signals to give T_2 weighting. All GE sequences must be constructed to avoid the formation of artefacts from coherence pathways (see Box 'Coherence Pathways').

Coherence Pathways

The analysis of coherence pathways is of prime importance to the sequence developer, but an understanding of coherence helps to know what the images are about and how the sequences perform. Every time an RF pulse occurs, magnetization will be flipped to both longitudinal and transverse planes resulting in a fresh FID, the possibility of echo formation and the storing of magnetization for later RF pulses to refocus. Figure 13.6 shows a so-called coherence pathway diagram which can be used to predict the echo-formation properties of trains of RF pulses. In the diagram, phase is represented vertically and time horizontally. For simplicity we only consider one component (sometimes called an 'isochromat') of the transverse magnetization rather than multiple vectors fanning out. The rules are simple. Every time there is an RF pulse the magnetization divides into three parts:

1. A part continues to dephase as if nothing had happened.
2. A part is converted to longitudinal magnetization which then does not further dephase and runs parallel to the time axis at constant phase.
3. Another part of transverse magnetization receives the opposite phase, and then continues to dephase (or 'rephase' if it's heading back towards the zero phase axis). Whenever one of the lines crosses the zero-phase axis you get an echo.

Figure 13.6 also shows how a stimulated echo is formed, first by converting the transverse magnetization to longitudinal by α_2, then inverting the phase with α_3 which converts it back to transverse magnetization. You can see that the diagram correctly predicts the existence and timing of the stimulated echo. When the pulse train is regular (i.e. $t_a = t_b$), the stimulated echoes will coincide with the spin echoes. The coherence diagram in Figure 13.6 does not show the effect of the imaging gradients, although these can also be included.

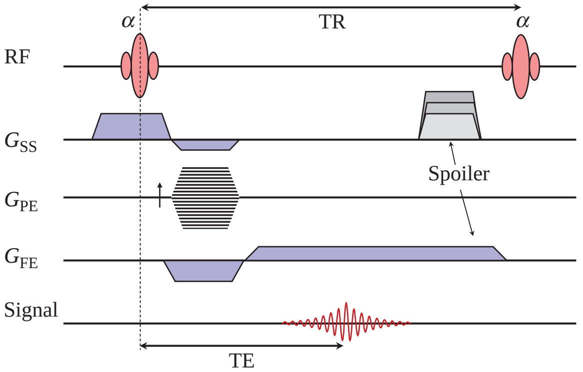

Figure 13.7 Spoiled gradient echo sequence utilizing gradient spoiling as a table on the slice-select gradient and a constant value on the frequency-encode axis and/or RF spoiling by varying the RF phase angle.

13.3.1 Spoiled Gradient Echo

In spoiled gradient echo only the FID signal, generated by the action of the current RF pulse on longitudinal magnetization, is utilized. The residual transverse magnetization remaining after the data-acquisition period (Figure 13.7) is removed by gradient spoiling, RF spoiling or both (see Box 'Spoil Sport'). In all other respects, the image-formation mechanism is conventional, with one line of k-space acquired per TR period.

The image contrast, mainly T_1W or PDW, is determined by TR and α, as was shown in Section 3.9. For each value of T_1 occurring in the image there is an optimum flip angle, known as the Ernst angle, that gives the most signal for a given TR. At flip angles greater than the Ernst angle you tend to get T_1 weighting. At less than the Ernst angle the contrast is flatter, more PD-like (Figure 13.8). With very low flip angles you can get pure PD weighting and also T_2^* weighting by increasing TE. A mathematical expression for the signal is given in Box 'Flash in the Pan: Signal Strength and the Ernst Angle'.

Flash in the Pan: Signal Strength and the Ernst Angle

The signal obtained from a spoiled GE sequence is

$$\text{Signal} = \rho \frac{\sin\alpha \cdot (1 - \exp(-\text{TR}/\text{T}_1)) \cdot \exp\left(-\text{TE}/\text{T}_2^*\right)}{1 - \cos\alpha \exp(-\text{TR}/\text{T}_1)}$$

and you can see that flip angle α is an important parameter in determining the image contrast as illustrated in Figure 13.8.

The Ernst angle for the maximum signal is given by

$$\alpha_{\text{Ernst}} = \cos^{-1}[\exp(-\text{TR}/\text{T}_1)]$$

Of course the Ernst angle can only be met for one value of T_1 in an image.

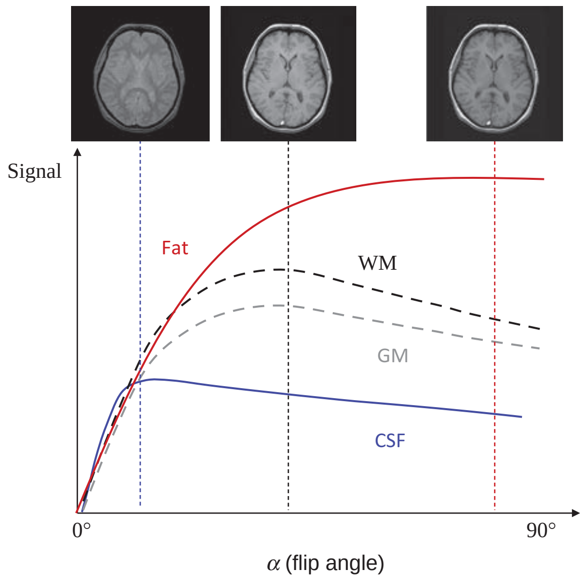

Figure 13.8 Signal intensity flip angle in spoiled GE, and image contrast below the Ernst angle, at the Ernst angle, for WM of above the Ernst angle.

Spoil Sport

Failure to spoil the transverse magnetization can result in two problems: the formation of image artefacts and wrong contrast. Image banding artefacts may also arise from incomplete spoiling, due to interference between differently phase-encoded signals from different excitations. A constant spoiling gradient will dephase only non-echo-forming parts of the signal. More thorough spoiling can be achieved by using a pseudo-randomly varying (i.e. the value isn't actually random, but the effect is) spoiler gradient table. Spoiler gradients can be applied on any axis, but the slice-select axis is commonly chosen as this represents the largest dimension of the voxel.

In RF spoiling we apply each α excitation pulse with a random or pseudo-random phase angle (direction in the rotating frame), as in Figure 13.9. The effect of this is to accentuate the natural dephasing of the spins, thus giving an apparent reduction in T_2 for the remnant of transverse magnetization from previous excitations.

Gradient spoiling (Figure 13.10a) must be sufficient to cause dephasing within a voxel, illustrated by the three lines. This effectively dephases any transverse magnetization that does not lead to a Hahn echo. However, it does not prevent echo formation. To avoid this, RF spoiling must be used (Figure 13.10b). Each RF pulse causes a vertical (phase) offset and if properly randomized the isochromats never add up constructively. The current FID signal is not affected. When RF spoiling is utilized the phase-encode gradients are usually rewound, otherwise unwanted spatial inhomogeneities in the signal can occur.

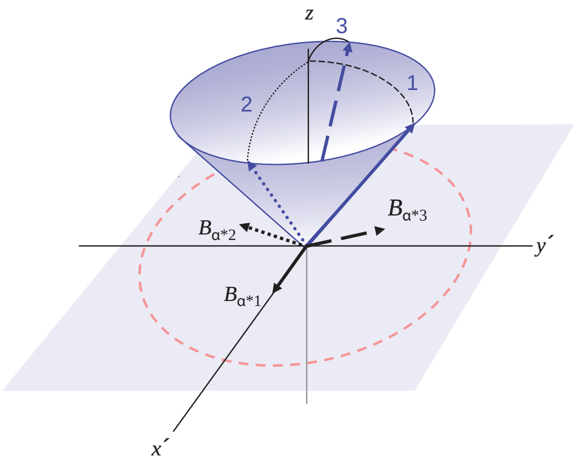

Figure 13.9 Principle of RF spoiling. Changing the RF phase changes the direction of the B_1 field in the rotating frame of reference. RF spoiling is denoted by the asterisks.

Gradient echo does not compensate for magnetic field differences. This includes dephasing from water and fat, which have slightly different resonant frequencies. Immediately after excitation, water and fat signals are in phase but precessing at different rates, seen as a dephasing over time in the rotating frame of reference. Once the two components get 180° out of phase with each other, the signals will subtract from one another. This does not affect the image, unless a voxel contains a mixture of water and fat, in which case a partial cancellation will occur. See Section 7.3.2 for a full discussion of this artefact and how to avoid it.

Alternatively, this feature can be utilized to provide information about the relative amounts of water and fat in tissues using in-phase/out-of-phase (IP/OP) GE. In the OP images, any voxels that contain both water and fat will have lower signal intensity than in the IP images. This is particularly noticeable at fat–water interfaces where partial volume means that voxels at the interface experience signal cancellation, giving a black line outlining the structure. IP/OP imaging is often used clinically to identify fat containing lesions such as adrenal adenomas. The IP/OP images can be acquired in a dual-echo GE sequence with breath-holding for abdominal imaging. These

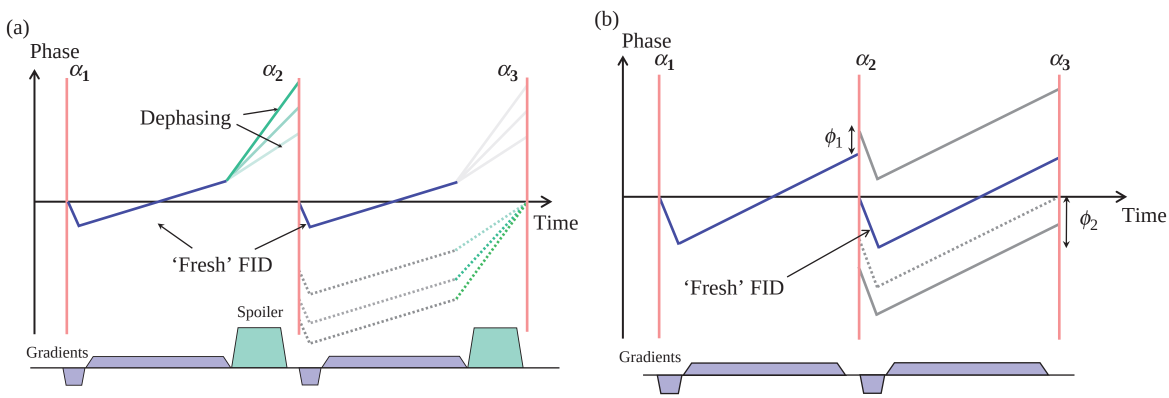

Figure 13.10 (a) Coherence diagram showing that gradient spoiling with a constant gradient amplitude dephases the non-echo-forming part of the FID, but that the echo-forming parts (dotted lines) are rephased. (b) Coherence diagram for RF spoiling showing that echo-forming and non-echo-forming parts of transverse magnetization do not form coherences. The dotted line shows the coherence pathway without RF spoiling. Fresh FID is considered to be 'in-phase'.

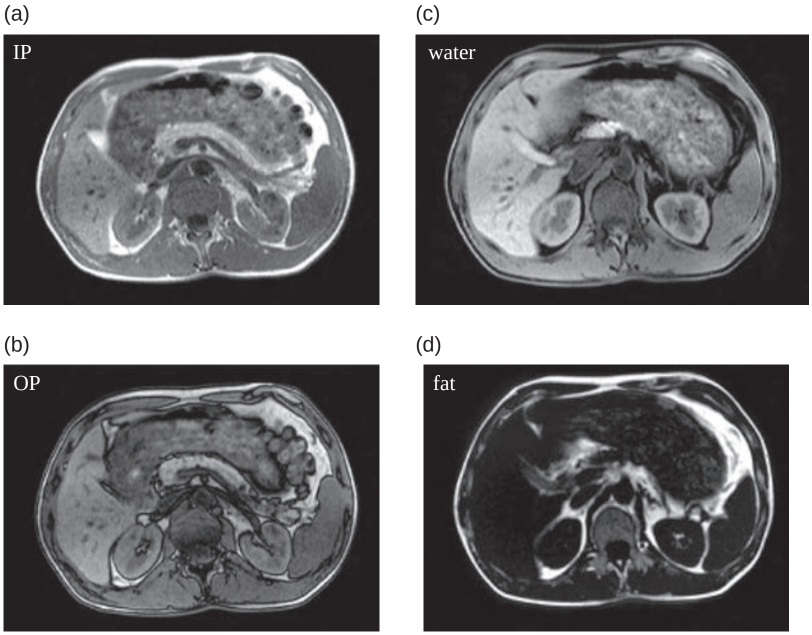

Figure 13.11 Dual in-phase (**a**) and out-of-phase (**b**) images together with calculated water (**c**) and fat (**d**) images using the two-point Dixon technique.

are often called two-point Dixon (2PD) methods and they can also be used to obtain images of water and fat as shown in Figure 13.11 and Box 'Two-Point Dixon Reconstruction'.

Two-Point Dixon Reconstruction

The IP/OP method described above is the basis of 'simple spectroscopic imaging' proposed by W. Thomas Dixon in 1984. Dixon's original method used two spin-echo acquisitions (and forms the basis of TSE-Dixon sequences), but here we apply it to GE.

The signal in the first echo OP image will be

$$S_{OP} = S_w - S_f$$

where S_w and S_f are the water and fat signals in a voxel. The second echo IP voxel signal will be

$$S_{IP} = S_w + S_f$$

From these we can calculate the water image from

$$S_w = 0.5(S_{OP} + S_{IP})$$

and the fat image as

$$S_f = 0.5(S_{OP} - S_{IP})$$

These are illustrated in Figure 13.11 and are good enough to give a subjective (i.e. radiological) assessment of the water and fat content of tissues. For fat quantification a more rigorous approach using a third echo to compensate for phase errors is required (see Chapter 19).

13.3.2 Rewound Gradient Echo

In coherent steady-state sequences, the transverse magnetization remaining after the signal-acquisition period is rewound, i.e. reset to zero by reversing the sign of the gradient pulses. In **F**ast **I**maging with **S**teady **P**recession (FISP) only the phase-encode gradient is rewound (Figure 13.12). Thus the signal contains FID enhanced with echo and coherent transverse components. This gives more signal than spoiled gradient echo but more complicated weighting. At longer TR values (>100 ms) and small flip angles there is little difference between spoiled and rewound gradient sequences. Also, if T_2 is short then there is little opportunity for enhanced contrast to develop from the coherent component. The ideal contrast behaviour depends only upon the flip angle and the ratio of T_2 to T_1, shown in Box 'On the Rewound'. As for spoiled sequences, the image-formation principles are completely conventional and the extension to 3D FT is standard, with the same equations for scan time applying.

Rewound GE produces good myelographic effect images. Figure 13.2b shows an example of rewound GE in the brain with bright CSF and little grey/white matter contrast. Since the signal is relatively independent of TR, rewound sequences are excellent for high contrast between fluid and solid structures in rapid imaging. However, because of the combination of

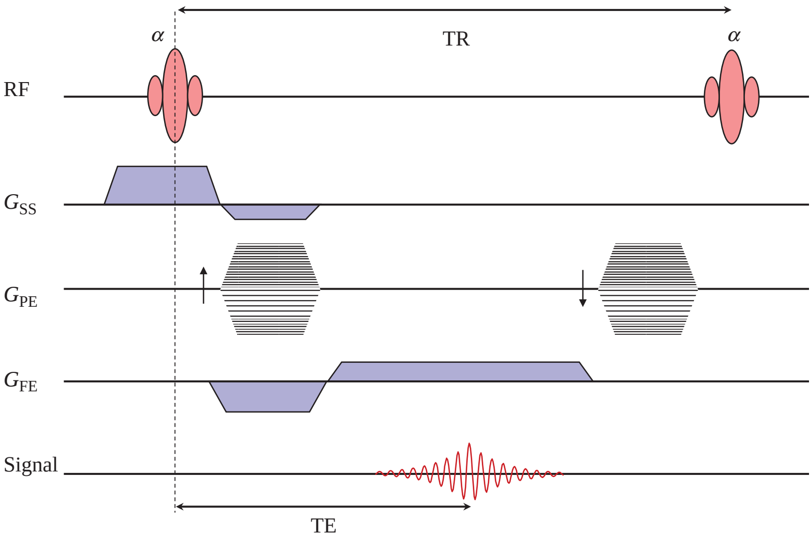

Figure 13.12 Rewound gradient-echo sequence. Only G_{PE} is rewound to avoid producing 'resonant offset' artefacts

refocused and fresh transverse magnetization, rewound GE sequences are sensitive to motion and flow, which can destroy the steady-state transverse coherence.

On the Rewound

A general solution for gradient-echo signal strength is

$$\text{Signal} = \rho \frac{\sin\alpha \cdot (1 - \exp(-\text{TR}/\text{T}_1)) \cdot \exp(-\text{TE}/\text{T}_2^*)}{1 - \cos\alpha \exp(-\text{TR}/\text{T}_1) - \exp(-\text{TR}/\text{T}_2) \cdot [\exp(-\text{TR}/\text{T}_1) - \cos\alpha]}$$

Rewound gradient-echo sequences (FISP, GRE, FFE, FAST) are used with very short TR, much less than T_1 and T_2. In this case the exponential terms can be approximated by Taylor expansions [e.g.exp(–TR/T_2) ≈ 1 – TR/T_2], and the above equation simplifies to

$$\text{Signal} = \rho \frac{\sin\alpha \cdot \exp(-\text{TE}/\text{T}_2^*)}{1 + \text{T}_1/\text{T}_2 - \cos\alpha(\text{T}_1/\text{T}_2 - 1)}$$

so the signal is ideally independent of TR, dependent only on flip angle and the ratio T_1/T_2. If $\alpha = 90°$ we get

$$\text{Signal} = \frac{\rho}{1 + \text{T}_1/\text{T}_2} \approx \frac{\rho \text{T}_2}{\text{T}_1}$$

if T_1 is much greater than T_2. As with spoiled gradient echo, there is a flip angle which gives an optimum SNR

$$\text{Signal}_{\text{opt}} \propto \sqrt{\frac{\text{T}_2}{\text{T}_1}}$$

sometimes quoted as the 'signal from true FISP'. Unlike spoiled GE sequences, however, the flip angle dependence is only moderate for most practical applications, e.g. imaging of fluids.

True FISP or balanced fast field echo (bFFE) is a sequence which has balanced, rewinding gradients in all three directions, as shown in Figure 13.13. An extension to 3D FT can be made by adding phase encoding and rewinding on the slice-select axis in place of the rephasing lobes. True FISP requires high-performance gradient technology to obtain a very short TR and good shimming. If this is not achieved the images become degraded with banding artefacts, which have spacing inversely proportional to the field inhomogeneity (see Box 'A Right ROASTing: Resonant Offsets'). Phase alternation of the RF pulse also helps to achieve a rapid steady-state magnetization and shifts these artefacts. True FISP has found clinical applications in cardiac imaging, where it provides excellent SNR and contrast between blood and the myocardium. Examples are shown in Chapter 16.

A Right ROASTing: Resonant Offsets

The main technical difficulty in true FISP arises from 'resonant offsets' (Figure 13.14). The number of RF excitations required to achieve a steady-state magnetization is dependent upon the amount of dephasing during TR. For spins that are not exactly on

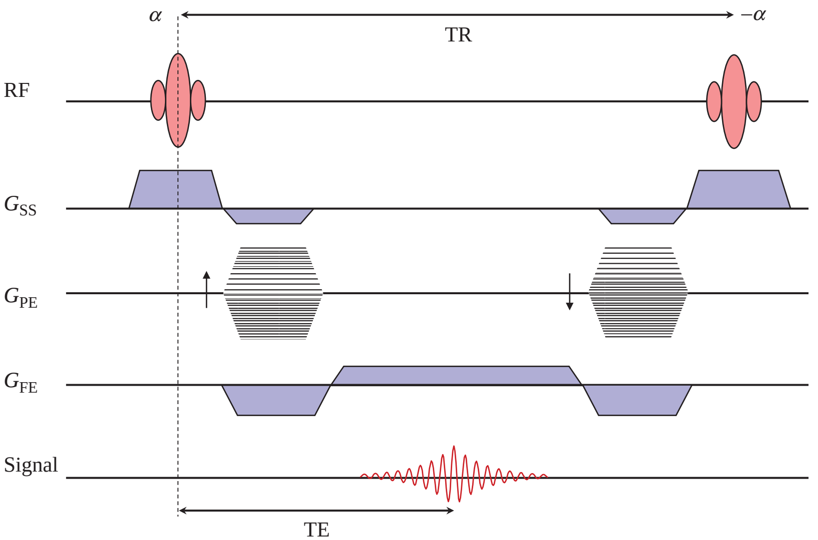

Figure 13.13 True FISP sequence. All gradients are balanced over one TR period.

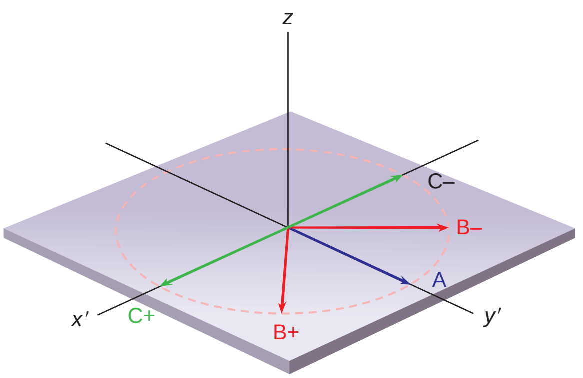

Figure 13.14 Resonance offsets. B_1 has maximum effect upon spins in orientation A, and no effect upon C. Only A is on resonance. In a fully balanced sequence, the spin orientations A, B and C would occur at different positions within the field of view, resulting in artefactual banding. In an unbalanced sequence the residual spread of phase angles from the imaging gradients will mask differences arising from field homogeneity.

resonance, e.g. due to main field inhomogeneities, the MR signal will oscillate from excitation to excitation, resulting in banding in the image related to the field inhomogeneity. A simple way of visualizing this is that progressive systematic errors are introduced to the flip angle. Phase-alternating the RF pulse can help to alleviate the problem, as does reducing TR. This problem only arises when all the gradients are balanced, e.g. in true FISP. In rewound sequences that are not fully balanced, the degree of residual dephasing is chosen to ensure that each voxel contains a full range of resonant offset angles and the problem is averaged out, i.e. each RF pulse will have the same effect. The term ROAST (**R**esonant **O**ffset **A**veraging **ST**eady State) is sometimes used to describe this technique

13.3.3 Echoes Only: Time-Reversed Gradient Echo

Gradient echo sequences that only utilize the echo component are known as time-reversed GE. An example is the oddly named PSIF sequence (try saying it after a few gins), an acronym that stands for nothing – but is FISP backwards both in spelling and in function! It is shown in Figure 13.15. Strictly speaking it is not a gradient-echo sequence as its signal is of Hahn echo origin. This is how it works: you start with the data acquisition, then you do the phase encoding and finally excite the signal! See Box 'If I Could Turn Back Time: How Time-reversed GE Works' for details. The images (Figure 13.2c) give a T_2-weighted appearance but with the advantage of a faster acquisition than spin echo. Time-reversed GE has the slightly odd property that the effective TE is approximately twice TR and that the degree of T_2 weighting is controlled mainly by adjusting TR. Its disadvantages are sensitivity to motion and relatively low signal-to-noise ratio (we are not using the majority of the signal at all). Time-reversed GE images are acquired in sequential mode (slice by slice) or 3D mode. Clinical

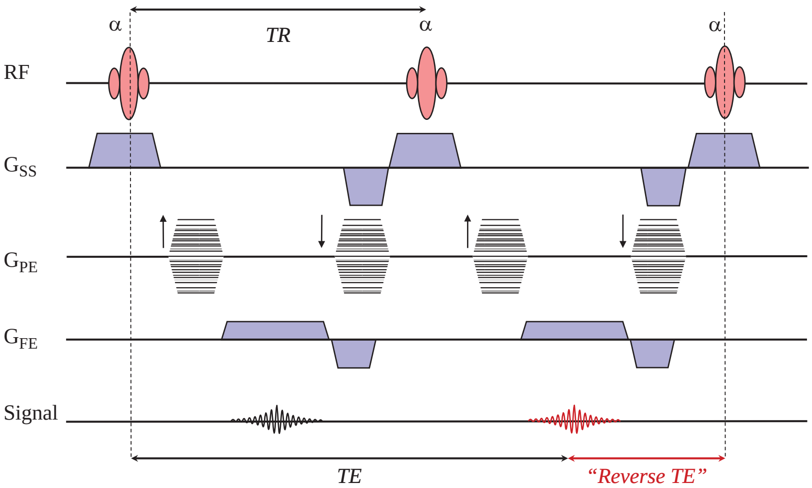

Figure 13.15 Time-reversed GE sequence. The first echo (shown in grey) occurs from an earlier TR period.

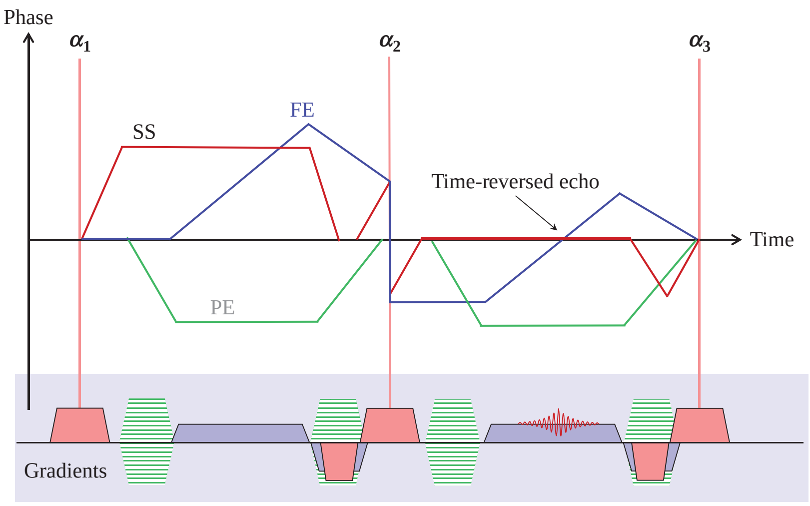

Figure 13.16 Coherence pathway diagram showing echo formation for time-reversed GE. The dephasing effect of each gradient is shown separately.

applications of time-reversed GE are few, but one is as an alternative to echo planar imaging for diffusion-weighted imaging.

If I Could Turn Back Time: How Time-Reversed GE Works

Figure 13.16 shows a coherence diagram for time-reversed GE. If we plot out the phase evolution for time-reversed GE we see that the first RF pulse causes the initial excitation of transverse magnetization, and this is dephased by the readout gradient and then partially rephased.

The second RF pulse flips the phase of part of this and the next readout gradient rephases this midway between the TR period to give the echo. Because two RF pulses are involved the behaviour is that of a Hahn echo, and hence T_2 weighted in nature. As in other coherent sequences, the phase encode requires rewinding. Slice selection is also rewound. As this is a time-reversed sequence, we often consider a 'reverse TE' (Figure 13.15) in which case the signal strength approximates to the following:

$$\text{Signal} \propto \exp\left(-\frac{2 \cdot \text{TR} - \text{TE}_{\text{reverse}}}{\text{T}_2}\right)$$

So the T_2 weighting is related to twice TR. For a short reverse TE we can say that the effective TE is approximately twice TR.

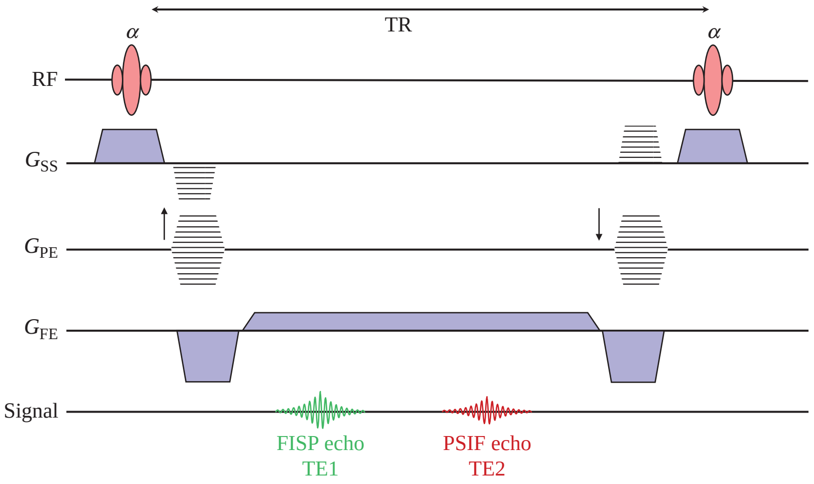

Figure 13.17 DESS sequence. The 'FISP' echo is the rewound gradient echo arising from the most recent RF pulse. The 'PSIF' echo is refocused from the previous excitation.

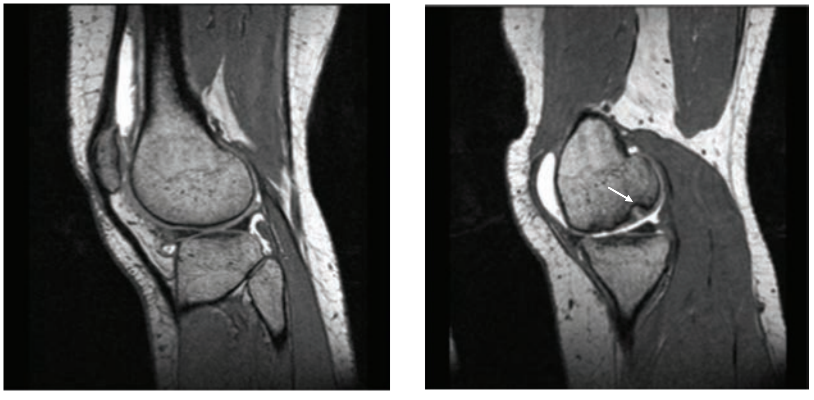

Figure 13.18 (a) DESS image of the sagittal knee showing bright fluid. (b) Cartilage defect and bone erosion (arrowed) shown by DESS. TR = 26.8 ms, TE = 9 ms, α = 40°.

13.3.4 Double Trouble: DESS and CISS

DESS (**D**ouble **E**cho **S**teady **S**tate) is a Siemens sequence in which two echoes are acquired, one a FISP gradient echo, the other a time-reversed (or PSIF Hahn) echo. The heart of the DESS sequence is shown in Figure 13.17. As this is primarily a 3D technique, phase encoding is applied on two axes after prior slab selection. The dephase and rephase portions are arranged such that the FISP echo occurs ahead of the PSIF echo. In the resultant image these two components are combined to give high-resolution images (the FISP part), with strong T_2 weighting (the PSIF part) giving strong fluid signals. DESS is quite sensitive to motion artefacts, but is well suited to high-resolution 3D orthopaedic scanning with spatial resolution at sub-millimetre dimensions, as shown in Figure 13.18.

CISS (**C**onstructive **I**nterference in **S**teady **S**tate), another Siemens sequence, is a combination of two true FISP images, one acquired with and one without alternating the sign of the RF pulses. The purpose of the sequence is to avoid banding artefacts that arise in true FISP when the TR is too long. It allows for very high-resolution GE images. State-of-the art gradient technology renders this sequence obsolete since we can now use 3D TSE instead.

13.4 Ultra-Fast GE Imaging

The GE sequences we have examined so far have utilized conventional spatial localization methods. In this section we look at sequences that use segmentation of k-space and non-steady-state methods in their image formation. This, combined with low flip angle techniques, enables them to run 'ultra-fast'. How fast

 https://doi.org/10.1017/9781107706958.014

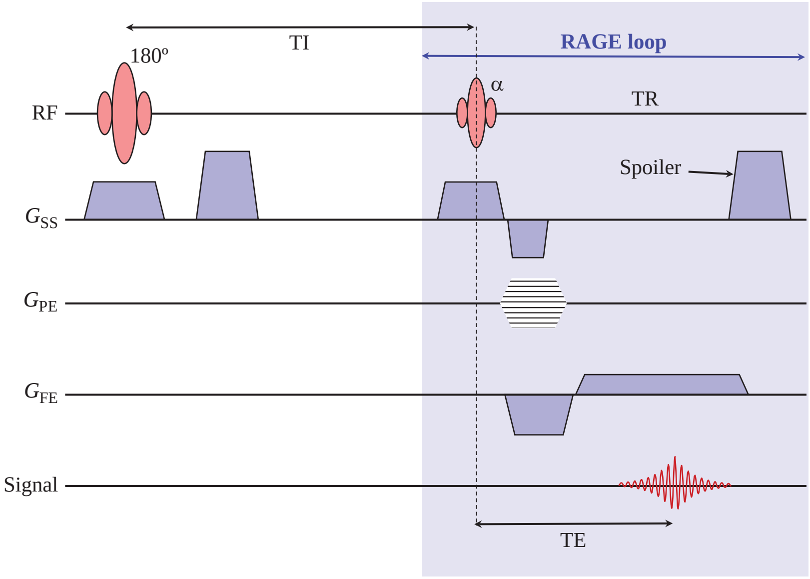

Figure 13.19 Turbo-FLASH sequence. An inverting prepulse and spoiler gradient precede the rapid acquired gradient echo (RAGE) loop for image formation.

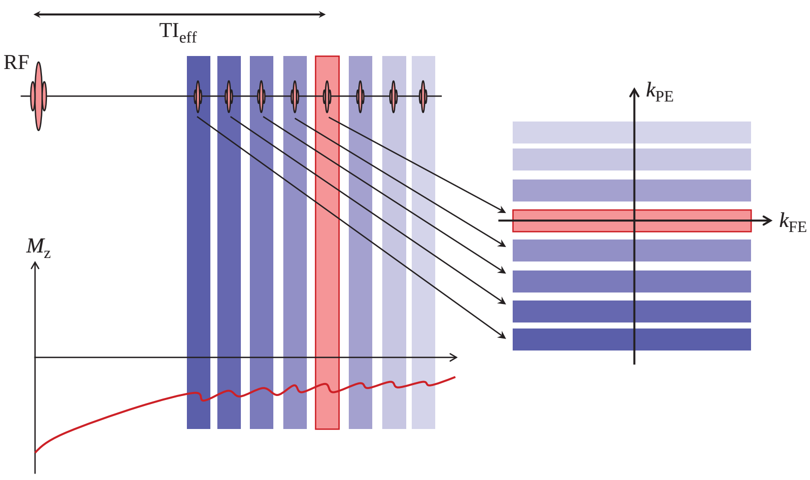

Figure 13.20 k-space acquisition for turbo-FLASH showing how the effective TI (TI_{eff}) occurs.

is ultrafast? How short is a piece of string? Generally scan times of a few seconds or less per whole slice used for dynamic studies.

13.4.1 Turbo-FLASH

Turbo-FLASH is a spoiled GE technique applied ultra-quickly with extremely short TR and very low flip angle. One of the consequences of a very short TR and low flip angle is that the T_1 contrast is very poor. To get round this problem, turbo-FLASH uses an inversion pre-pulse followed by a delay to generate T_1 weighting as shown in Figure 13.19. As for TSE, the order of phase encoding affects the contrast, with an effective inversion time TI from the centre of the inversion RF pre-pulse to the centre of k-space shown in Figure 13.20. For a linear-ordered phase encoding this is

$$TI_{eff} = TI + \frac{N_{PE}}{2} \cdot TR$$

Therefore with this sequence changing the matrix size (in the phase-encode direction) changes the contrast.

On most scanners the definition of TI has been changed to be the time from the initial inversion to the middle of k-space (Figure 13.20). This makes much more sense as now you don't change the contrast if you change the matrix size; instead the scanner

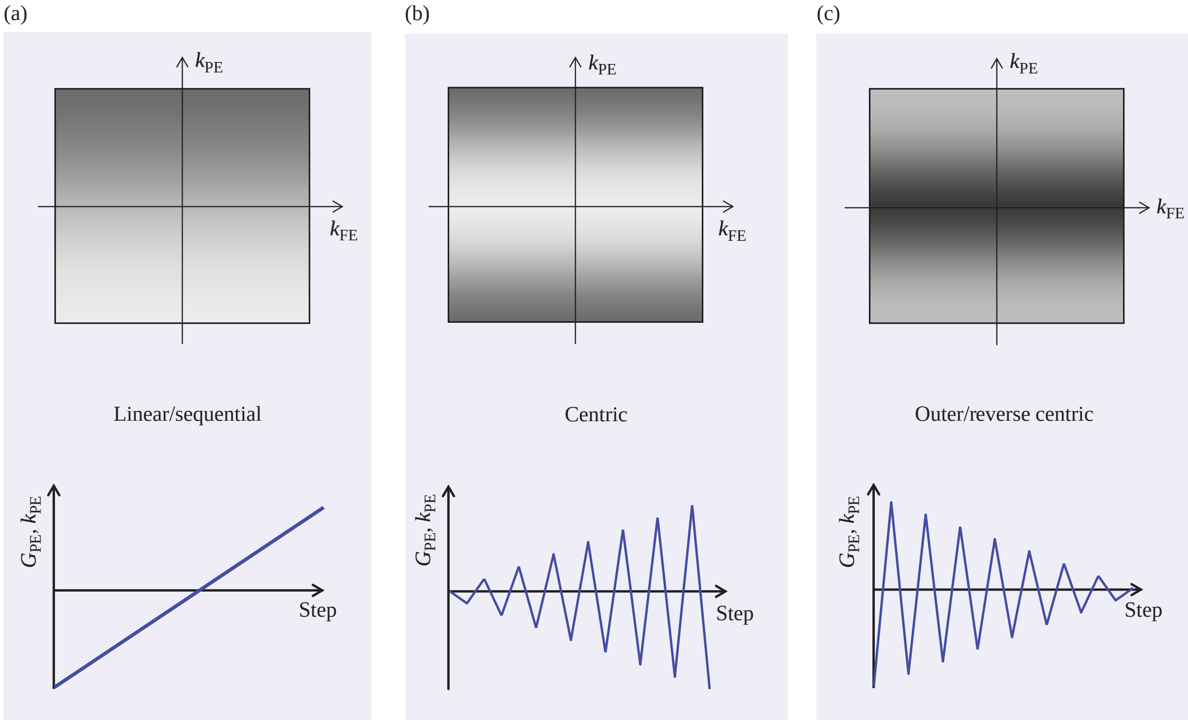

Figure 13.21 k-space ordering schemes: (**a**) linear or sequential, (**b**) centric, (**c**) reverse-centric. In centric the image contrast is determined by the beginning of the acquisition, in reverse centric by the end.

adjusts the delay between the inversion pulse and the start of the RAGE loop to give the desired TI.

Turbo-FLASH can run very fast, acquiring a whole slice in 1 or 2 s. When used in a multiple-slice mode, it is applied sequentially. That is, the whole of one slice is acquired before the next. A delay, TD, between slice acquisitions must be applied if a non-selective inversion pulse is used. The scan time is therefore proportional to the number of slices:

$$\text{Scan time} = N_{\text{slices}} \times (\text{TI} + N_{\text{PE}} \cdot \text{TR} + \text{TD})$$

Turbo-FLASH can be applied in both single-shot and segmented mode. In single-shot mode the whole of k-space is acquired by the train of RF pulses. This imposes practical limits on the spatial resolution achievable but makes for very rapid (1 s per slice) acquisitions. In segmented turbo-FLASH k-space is divided into segments and the whole sequence repeated a number of times. Typically up to 32 lines of k-space may be acquired per shot. In order to avoid jumps in signal intensity from one segment to the next, interleaving schemes may be employed. Furthermore, the ordering of phase-encode steps affects the contrast as shown in Box 'k-space Ordering Scheme'.

k-Space Ordering Scheme

In standard spin-echo imaging the order in which the lines of k-space are acquired is generally from maximum negative to maximum positive (or vice versa). This is called linear or sequential ordering. In spin echo the actual order does not matter, as the underlying signal does not change from line to line. The order does matter for segmented k-space and single-shot sequences.

Another commonly used order is centric, where the lowest k_{PE} values are measured first with positive and negative values alternating, i.e. 0, −1, 1, −2, 2, . . ., $-N_{PE}/2$, $N_{PE}/2$. This will result in contrast dominated by the beginning of the acquisition period.

Reverse or outer centric is similar but starts from the large values and works backwards. Image contrast will be dominated by the end of the acquisition. These are illustrated in Figure 13.21.

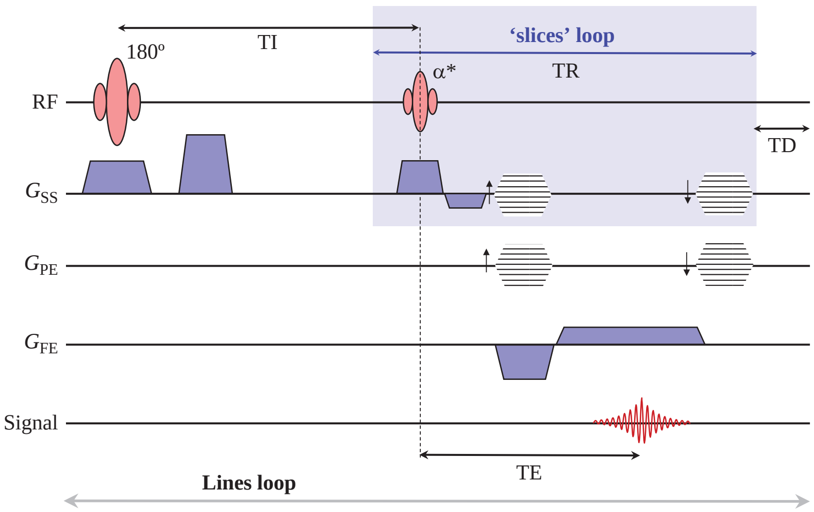

Figure 13.22 3D MP-RAGE sequence. Note that when RF spoiling (denoted by asterisk) is deployed the phase-encode gradients are rewound.

The turbo-FLASH sequence involves RF spoiling to avoid contamination of T_1-weighted contrast by T_2 effects. It is, however, different from spoiled gradient echo in that a steady state is not achieved during data acquisition. The magnetization exists in a transient state, undergoing repetitive very small flip angles while the longitudinal relaxation is recovering from its initial inversion. By appropriately varying the flip angle during the readout portion of the sequence, oscillations of magnetization and, subsequently, inconsistencies of k-space data can be avoided.

Turbo-FLASH is also known as IR-FSPGR (on GE Healthcare scanners) or sometimes T_1-Turbo-FLASH. It is also possible to have T_2-Turbo-FLASH (DE-FSPGR on GE Healthcare systems), which as the name suggests gives T_2-weighted images. This is achieved by replacing the inversion pulse with a 90°–180°–90° set of preparation pulses. The 90°–180° pair produces a T_2-weighted spin echo, which is returned to the z axis by the second 90°. The turbo-FLASH loop immediately follows to produce the image, so 'TI' now defines the amount of T_2 weighting.

13.4.2 MP-RAGE

MP-RAGE or **M**agnetization **P**repared **R**apid **A**cquisition by **G**radient **E**cho is the same in principle as turbo-FLASH. However, the name has tended to apply to a particular 3D implementation of turbo-FLASH shown in Figure 13.22. As a 3D technique there are too many combinations of the two phase-encode gradients to acquire the whole of 3D k-space from a single preparation. The solution is to acquire all the 'slice' encoding lines of data from each prep, then introduce a recovery delay (as in segmented turbo-FLASH) before moving on to the next in-plane line of k-space. As a result the in-plane resolution is not compromised, the data being all acquired with the same degree of relaxation. MP-RAGE can produce very high-resolution, T_1-weighted images showing very good anatomical detail, particularly of the brain (Figure 13.23). The introduction of this delay means that MP-RAGE is not ultra-fast in its scan time (although it uses ultra-fast methods). The scan time is

$$\text{Scan time} = \text{NSA} \times N_{\text{PE}} \times (N_{\text{slices}} \cdot \text{TR} + \text{TI} + \text{TD})$$

13.4.3 Other Ultrafast GE Sequence Variations

It has become commonplace for MR manufacturers to offer anatomy- or application-specific optimized GE protocols. For example, VIBE, LAVA or THRIVE are 3D gradient-echo sequences with optimized k-space coverage and interpolation, all intended for imaging of liver in a breath-hold. The contrast behaviour follows that of a T_1-weighted spoiled gradient echo (Figure 13.24).

An extension of the 3D-optimized k-space GE approach is to combine 3D imaging with radial acquisition in a stack of 2D planes, the so-called 'stack of stars' (Figure 13.25). Two-dimensional radial scanning utilizes two simultaneous gradients for the frequency encoding with amplitudes varying to produce a range of angles in k-space. One advantage is immunity from

 https://doi.org/10.1017/9781107706958.014

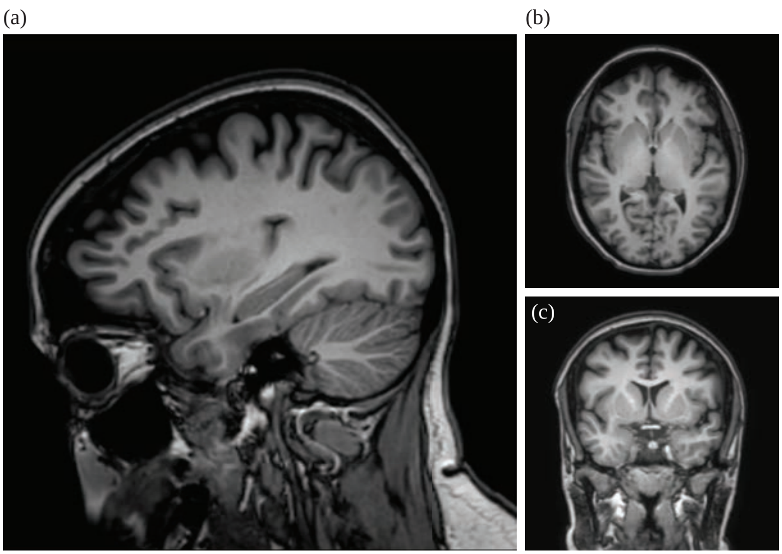

Figure 13.23 Multi-planar reformatted high-resolution 3D T_1-weighted MP-RAGE images: (**a**) transverse, (**b**) sagittal, (**c**) coronal.

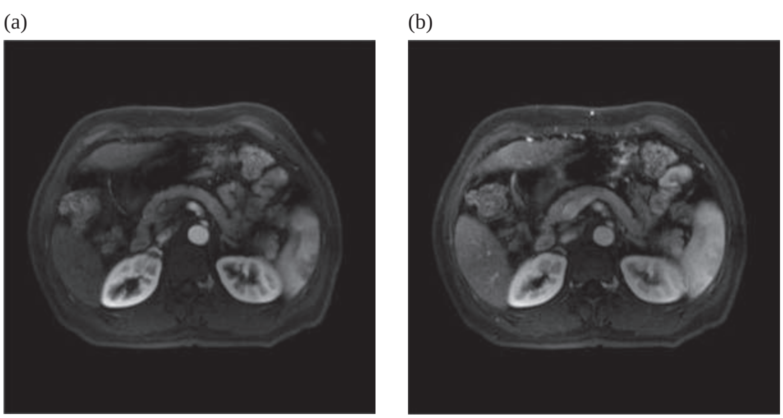

Figure 13.24 VIBE images: (**a**) arterial phase, (**b**) venous phase.

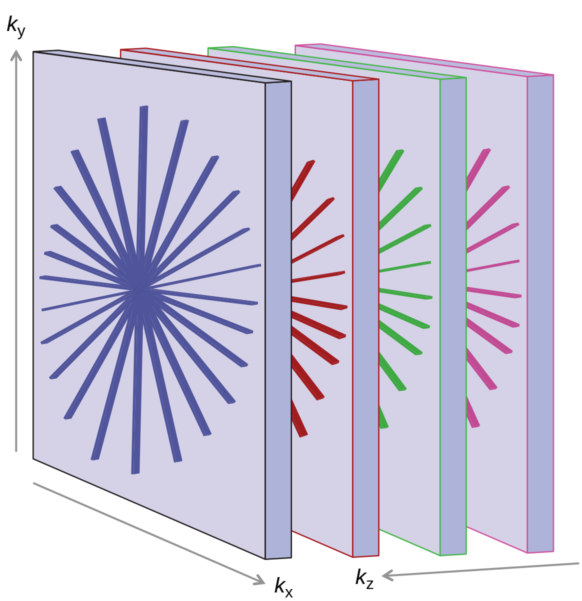

Figure 13.25 k-space for 'stack of stars'.

phase-wrap since the only phase encoding occurs in the slice-selective direction. Small FOVs can easily be acquired. A second advantage is that the continual sampling of the centre of k-space allows for motion correction (as was the case for PROPELLER). It also allows for a finer sampling of the centre of k-space than the edges, good for interpolation and for keeping the scan time down. Further details on radial and other non-Cartesian acquisitions are contained in Section 14.8. The stack of stars sequence has been implemented as Star-VIBE on Siemens scanners.

13.4.4 GE Echo Planar Imaging

Echo planar imaging (EPI) is the fastest pulse sequence, capable of producing a whole slice in under 100 ms. In single-shot GE-EPI the whole train of gradient echoes are acquired following a single RF excitation pulse (Figure 13.27). In this instance, the phase encoding of each line is acquired by adding a

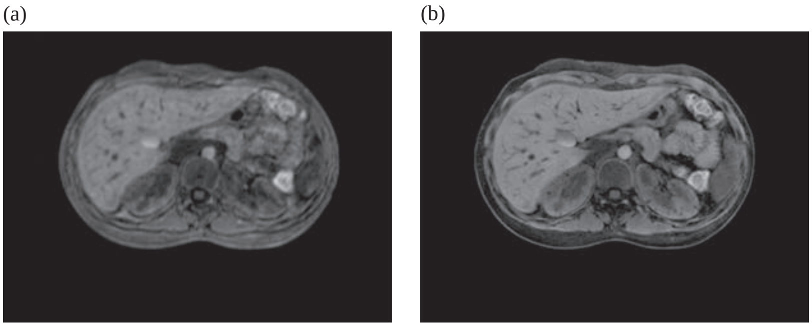

Figure 13.26 (a) conventional VIBE image, (b) Star-VIBE image. Courtesy of Siemens Healthcare.

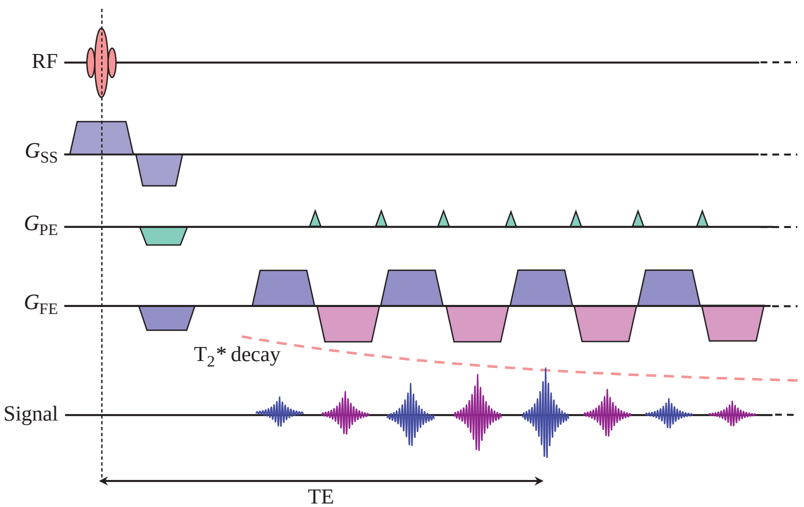

Figure 13.27 'Blipped' single-shot GE-EPI sequence. In practice 64–128 echoes would be used.

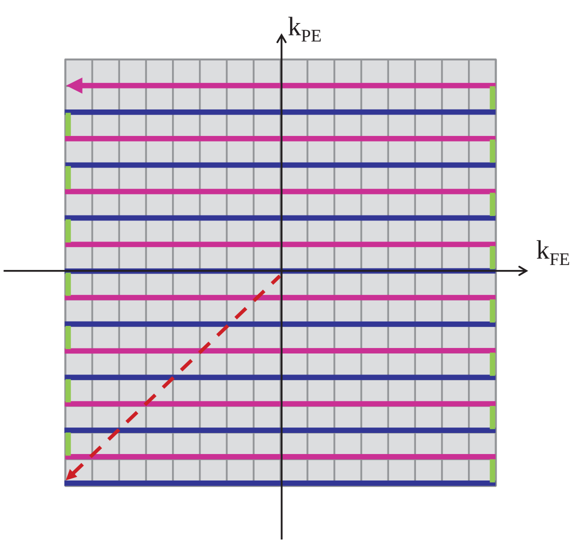

Figure 13.28 k-space trajectory for gradient echo EPI.

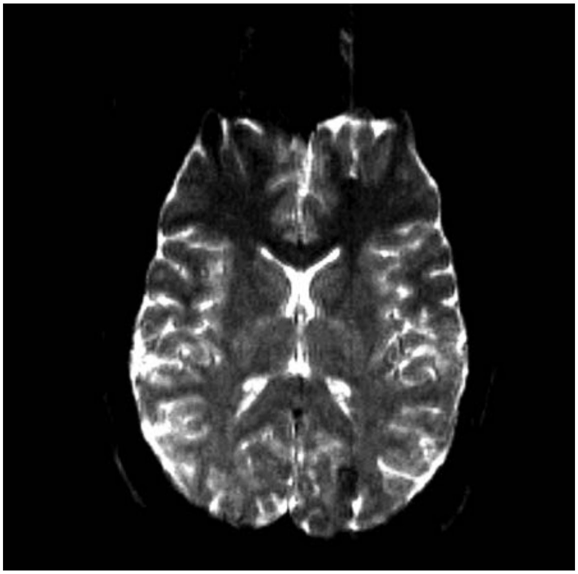

Figure 13.29 Gradient echo EPI image used for BOLD 'brain activation' imaging.

constant-amplitude gradient lobe, or 'blip', after each frequency-encode gradient reversal. Figure 13.28 shows the corresponding k-space trajectory.

GE-EPI consists of a lengthy series of gradient echoes, symmetrical about the centre of k-space. This results in a relatively long (effective) TE and the image contrast of GE-EPI is consequently T_2^*-weighted and exhibits a strong sensitivity to susceptibility variations (Figure 13.29). This, together with its speed, makes it the sequence of choice for BOLD (**B**lood **O**xygenation **L**evel **D**ependent) fMRI studies, considered in Chapter 18.

To run successfully, EPI requires high-performance gradients. EPI suffers from a number of inherent limitations in image quality, including relatively low spatial resolution and spatial distortions. GE-EPI artefacts are similar in nature to those from the spin-echo variant, considered in Section 12.5.3.

An alternative approach to imaging tissue susceptibility differences is SWI (**S**usceptibility-**W**eighted **I**maging). This yields high-resolution 3D images that are sensitive to small vessels and micro-bleeds in the brain. See Chapter 15 for details and clinical usage of SWI.

See also:

- How frequency- and phase-encoding gradients work: Chapter 8
- Basic image contrast: Chapter 3
- Pulse sequences for angiography and cardiac imaging: Chapters 15 and 16.

Further Reading

Bernstein MA, King KF and Zhou XJ (2004) *Handbook of MRI Pulse Sequences*. London: Elsevier Academic Press.

Brown MA and Semelka RC (1999) 'MR imaging abbreviations, definitions and descriptions: a review'. *Radiology* 213:647–662.

Brown RW, Cheng YCN, Haacke EM, Thompson MR and Venkatesan R (2014) *Magnetic Resonance Imaging: Physical Principles and Sequence Design*, 2nd edn. Hoboken, NJ: John Wiley & Sons, chapters 18 and 26.

Elster AD and Burdette JH (2001) *Questions and Answers in Magnetic Resonance Imaging*, 2nd edn. London: Mosby-Yearbook, chapters 5 and 12. Also on the web at http://mri-q.com [accessed 23 March 2015].

Haacke EM and Tkach JA (1990) 'Fast MR imaging: techniques and clinical applications'. *Am J Roentgen* 155:951–964.

Liney G (2011) *MRI from A to Z*, 2nd edn. London: Springer-Verlag.

Mansfield P and Maudsley AA (1977) 'Medical imaging by NMR'. *Br J Radiol* 50:188–194.

Twieg DB (1983) 'The k-trajectory formulation of the NMR imaging process with applications in analysis and synthesis of imaging methods'. *Med Phys* 10:610–623.